Heritage Science

RESEARCH

Open Access

New solidification simulation reveals the secret of the hidden metal cores in ancient Chinese bronzes

Huan Yang[1*], Minghui Fang[2], Yihang Chang[3], Ruiliang Liu[4], Zhao Fang[2] and Junchang Yang[1]

Abstract

Regardless of the tremendous number of studies on ancient Chinese bronzes and fruitful understanding of the raw materials, technologies and their cultural significance, many related issues have still not been tackled. In particular, it has been known for decades that the legs of Shang and Zhou bronzes have metal cores, but their specific function remains ambiguous. In this work, the Finite Element Method is applied to simulate the pouring and solidification process of bronze cores of different sizes. The findings illustrate that throughout the casting process, the metal core not only maintains the uniformity of the bronze and reducing its's wall thickness but also lowers the temperature of the surrounding alloy liquid, serving as a casting chill. Specifically, the metal core allows elimination of over 60% of casting defects. In comparison with more widespread clay cores, metal cores help produce less shrinkage porosity, therefore prevent cracking of the legs that is usually caused by different shrinkage rates between the clay core and the metal wall. In summary, the use of metal cores in ancient Chinese bronzes reveals a deep knowledge about the metal properties and the solidification process since the Chinese late Shang period (ca. 1250–1045 BC).

Keywords Bronze tripod, Metal core, Solidification process simulation, Chill, Casting defects

Introduction

Bronzes are among the most important categories of objects in Shang and Zhou dynasties of China (about 1600–221BCE) [1]. Since the 1930s, a large number of studies have been conducted to elucidate the casting technologies in ancient Chinese bronzes [2, 3]. With the emergence of various scientific methods, the complexity of bronze casting technology has been progressively disentangled, especially with the help of X-ray and CT detection tools. X-ray methods have been applied to investigate cultural relics since the 1920s, and their first use with respect to ancient Chinese bronzes was reported in the 1970s [4]. More details about the internal and external structure of bronzes and casting defects have become available due to computed tomography (CT) in the 21st century [5].

One of the most vital challenges concerning bronze casting is to eliminate casting defects. Such defects are usually caused by hot spots that appear in the solidification process of a crystalline metal structure [6, 7]. For example, in the case of a ritual vessel tripod, the casting hot spots are mainly concentrated in solid handles and legs. This is because of their much larger thickness compared to the remaining parts of the tripod, which requires longer time for solidification [8]. In modern industry, chill serves to promote solidification in a specific portion

*Correspondence:
Huan Yang
yanghuan2019@nwpu.edu.cn
[1] Institute of Culture and Heritage, Northwestern Polytechnical University, 127 West Youyi Road, Beilin District, Xi'an 710072, Shaanxi, People's Republic of China
[2] School of Materials Science and Engineering, Northwestern Polytechnical University, 127 West Youyi Road, Beilin District, Xi'an 710072, Shaanxi, People's Republic of China
[3] School of Ecology and Environment, Northwestern Polytechnical University, 127 West Youyi Road, Beilin District, Xi'an 710072, Shaanxi, People's Republic of China
[4] British Museum, Great Russell Street, London WC1B 3DG, UK

of a casting mold and to eliminate hot spots [9–11]. In the current research, we argue that ancient craftsmen realized this issue in casting for a long time and one of the early solutions was placing a metal core inside a specific location of the vessel to reduce or eliminate hot spots and improve casting quality.

Based on the long-term research on ancient Chinese bronze casting technology, it was concluded that most of the hollowed parts of bronze in Shang and Zhou periods comprised clay cores [8]. However, since the end of the 21st century, the presence of metal cores inside the legs of several tripods dated to the late Shang and early Zhou periods (ca. 1250–975BCE) has attracted scholarly attention. The metal cores were first described in detail by Meyers [12] upon examination of legs of a bronze ritual vessel in the Sackler Art Museum, related to the late Shang dynasty period (ca. 1250–1045BCE). He suggested that the copper content of the metal core was about 98%, basically pure copper [12].

According to Meyers, the use of metal cores suggested a clear awareness of the difference between melting points of alloying elements by the craftsmen and the need to reduce casting defects. Moreover, atomic absorption spectroscopy analysis of the composition of these tripod vessels showed very low levels of lead (below 3.3%) [12]. Liu Ruiliang's research revealed a significant correlation between the alloy composition of ancient bronze and social hierarchy. The bronze materials and components possessed by the higher elites exhibit superior quality, while those owned by the lower elites may have originated from recycling or mixing, resulting in substantial variations in impurity element content [13]. At the same time, according to Yanghuan, the minor lead content could also indicate that vessels might have belonged to a higher rank master [14].

The use of metal cores was also mentioned by Chase, who believed that it was an important advance in metal casting technology during the late Shang Dynasty period. The metal cores were generally made of copper and placed in the legs of the tripod to prevent hot tearing and shrinkage caused by the wall thickness irregularity of the solid objects upon their solidification [15].

Lian Haiping also found metal cores in the legs of four bronze tripods stored in Shanghai Museum, which were reliably dated to the late Shang Dynasty period and the early Western Zhou Dynasty era (ca. 1045–975BCE) (Fig. 1a–c, e). Based on a careful examination of these bronzes, their casting process was concluded to be as follows. Three metal cores with tenons were inserted into the leg mold cavities of the vessel to be afterward integrated with the tripod by casting. The clearly identifiable edges of metal tenons can be observed on the

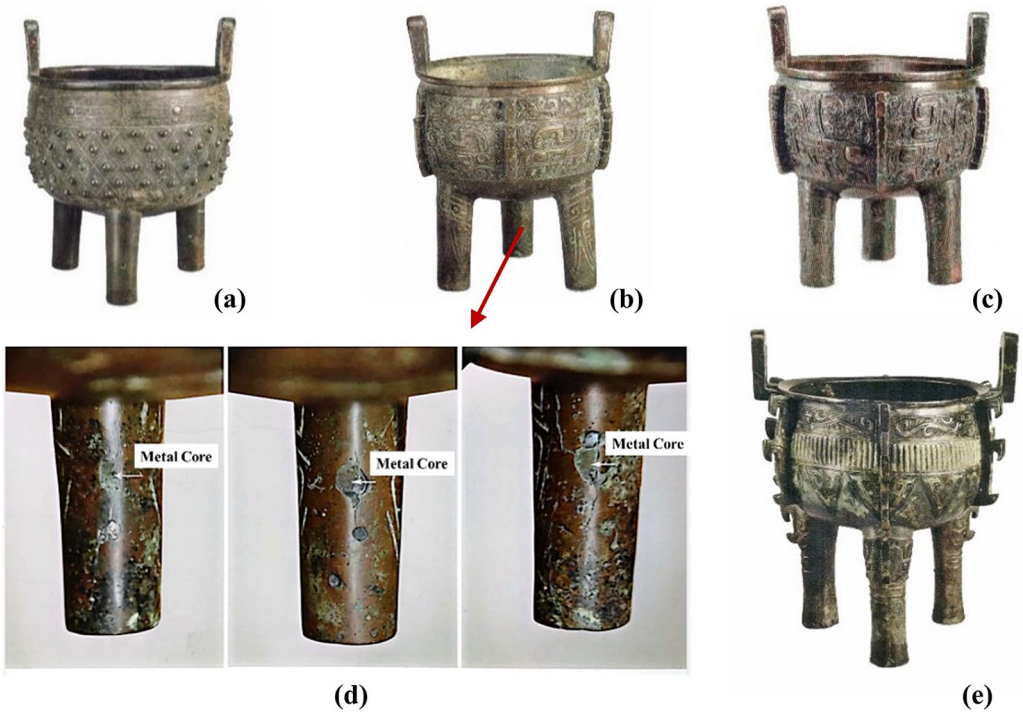

Fig. 1 Four bronze tripods stored in Shanghai Museum with metal cores in the legs (**a** Zixiejunqi Tripod. **b** Shi Tripod. **c** Ge Tripod. **d** Metal cores in three legs of Shi Tripod. **e** Chuan Tripod)

inner surface of the legs of the *Shi Tripod* dated to the late Shang Dynasty period, which is kept in Shanghai Museum (Fig. 1d). According to Lian et al., the material of the metal core is pure copper or bronze with higher copper content than the body [16]. The detection also revealed that tripods were obtained via exquisite casting with subsequent fine polishing, indicating brilliant fabrication crafts.

Due to the lack of systematic research on metal cores, the understanding of metal cores and the underlying engineering mechanisms as well as social implications are quite limited. In fact, the discovery of metal cores raises many questions when exploring ancient Chinese bronze casting techniques. First of all, the specific function of the metal core is unknown, such as the extent to which casting defects can be eliminated. Another curious fact concerns the main functions of bronze casting technology itself; in particular, the advantages of metal cores over those of clay cores [17]. Furthermore, it is interesting to know how the optimal size of metal cores could be achieved. These problems are related to the technical motivation for using metal cores by craftsmen in the Shang and Zhou periods and undoubtedly merit thorough study.

Numerical simulation methods can simulate the effects of different casting system designs on temperature gradient, cooling rate, solidification process, etc. [18]. In order to clarify the role of metal core in casting, the Finite Element Method (FEM) was employed in this work for stepwise reconstruction of the solidification process and elimination of casting defects. ProCAST software, on the basis of finite element simulation, is widely used in materials and engineering sciences [7, 19, 20]. This method allows accurate prediction of the macroscopic and microscopic structures and casting defects in vessels through dynamic recording of the solidification process [21, 22].

Three-dimensional modeling of bronze and clay molds (cavities) was performed, and the thermal and physical parameters of molds were calculated and measured at the same time. Then, the mold flow simulation of casting and solidification processes of a bronze tripod was carried out [6]. In the simulation, the size of the metal core was set as a variable, and the optimal size of the metal core was determined through continuous attempts. The effect of the optimal size of the metal core on casting performance was then compared with that of the clay core of the same dimensions to clarify the action mechanism and advantages of the former material.

Simulation conditions and process

Simulation setting

The rationale of FEM is to discretize the computational domain into multiple sub-computational domains through geometric processing and mesh division of the CAD model. These computational domains are interconnected at nodes, and physical quantities in each domain can be obtained by their interpolation on nodes [23]. ProCAST (ESI Group, France)was chosen for simulation based on FEM numerical simulation method. This approach finds wide application in industry due to its high accuracy [24].

The vessel tripod was taken as the simulation object. Before solidification simulation, it is necessary to observe the clay mold unearthed from the foundry, in order to conduct 3D modeling of its cavity (Fig. 2). The research model in this article was created and corrected by ProE in CAD.Metal cores of different diameters were designed to assess their impact on bronze casting. In addition, a control blank without cores was simulated (referred to as Group (A) in Table 2). When the physical model is simplified, the quality of automesh can be improved with the utilization of the MeshCAST module in ProCAST. Smaller mesh size and higher number of mesh elements will increase simulation accuracy. However, when the number of mesh elements reaches a certain value, the calculation time will increase but the simulation accuracy will not be greatly increased. Combined accuracy and efficiency, tria mesh type was prudently chosen in our research to conduct further process. After automesh using MeshCAST, it is checked that there are no bad elements and negative Jacobian elements (Neg-Jac). With a mesh size of 6 mm for clay molds and a mesh size of 2 mm for the casting, as well as 1 mm for the metal cores and chaplets, the simulation accuracy and calculation time requirements can be guaranteed at the same time. Ultimately, the model has around 100,000 2D mesh elements and around 2 million 3D mesh elements (Fig. 2) [25].

According to external dimensions of the unearthed bronzes and the metal component proportion of each part, a suitable bronze tripod model was further established. The specific dimensions were set as follows: the total height of 215 mm, the leg diameter of 20 mm, and the leg height of 70 mm. The outer diameter of the rim was 160 mm, and the rim folded 8 mm along the outside. The tripod ear was U-shaped and 30 mm high. The thickness of the body wall was 3 mm (Fig. 2). The body was composed of 89% Cu, 10% Sn, and 1% Pb. There were six chaplets in the cavity to ensure the cavity space; the size of the chaplets was 5 mm, and their composition was 95% Cu, 3% Sn, and 1% Pb (Table 1). The liquidus temperature of $Cu_{89}Sn_{10}Pb_1$ is 989.2 °C, and the solidus temperature is 676.5 °C. The initial pouring temperature of the clay mold is room temperature. The casting conditions for this model are gravity

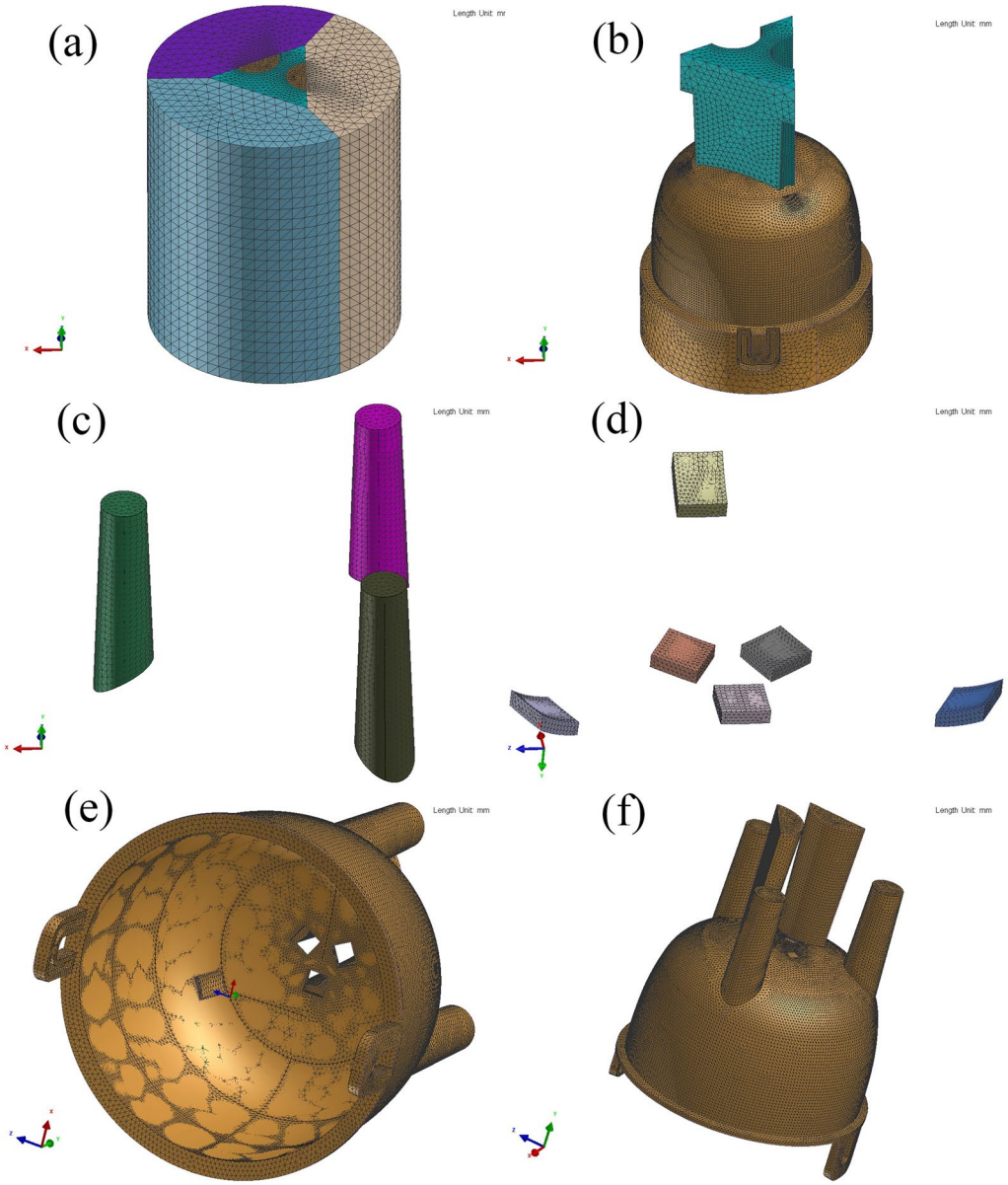

Fig. 2 Model and surface mesh (**a** entirety, **b** inner core, **c** metal cores, **d** chaplets, **e** inner surface, **f** outer surface)

casting and air cooling. After about ten minutes, the casting is taken out of the mold cavity by the craftsman.

In the simulation software for solidification, the configuration of simulation parameters holds paramount importance. This experiment encompasses the physical property parameters of both metal alloys and clay molds. The parameters for metals are automatically generated by the system database upon specifying the alloy composition, including thermal conductivity, density, enthalpy, fraction solid, and viscosity (Fig. 3). For the clay mold parameters, since the ancient cavity parameters are absent in the database, this study focuses on the clay molds unearthed from the Zhouyuan Zhuangli Foundary as the subject of investigation, involving the measurement and computation of thermal and physical properties. Specifically, these properties include specific heat capacity, density, thermal conductivity, and interfacial heat transfer coefficient. Due to the complexity of theoretical calculations involved in this research, a separate article has been composed, which is scheduled for publication in the near future.

Table 1 Specific dimensions and composition of the sample tripod (dimension: mm; Cu, Sn, Pb: wt%)

Location of sample	Type of dimensions	Dimensions	Cu	Sn	Pb
The total body	Height	215	89	10	1
Leg	Diameter	20			
	Height	70			
Rim	Outer diameter	160			
	Folded along the outside	8			
Handle (ear)	Height	30			
Body wall	Thickness	3			
Chaplets	Size	5	95	3	1

Simulation process

Some studies have indicated that the size of the chilled iron, such as its thickness, has an impact on the casting defects [26]. After the construction of the model, the whole solidification process was reproduced in the ProCAST software by setting different diameters of the metal core (Table 2). The entire process from the beginning of pouring until the last second of solidification in a dynamic manner can be observed in Fig. 4. During simulation, the hot spots and shrinkage porosities can be clearly distinguished at various metal core diameters.

Among these parameters, the change in solidification time can alter the microstructure of the specific parts. A secondary dendrite arm of the bronze leg was modeled using the Furer–Wunderlin formula to observe the optimization effect of the metal core on the microstructure of the bronze [27]. At the end of the experiment, a comparative study was performed to evaluate the volume of shrinkage porosities between metal and clay cores, so as to obtain a deeper understanding of this technology from the perspective of materials science [28].

$$\lambda_2 = 5.5\left(At_f\right)^{\frac{1}{3}} \tag{1}$$

where λ_2 refers to the secondary dendrite arm spacing and t_f is the solidification time of a particular part of the casting.

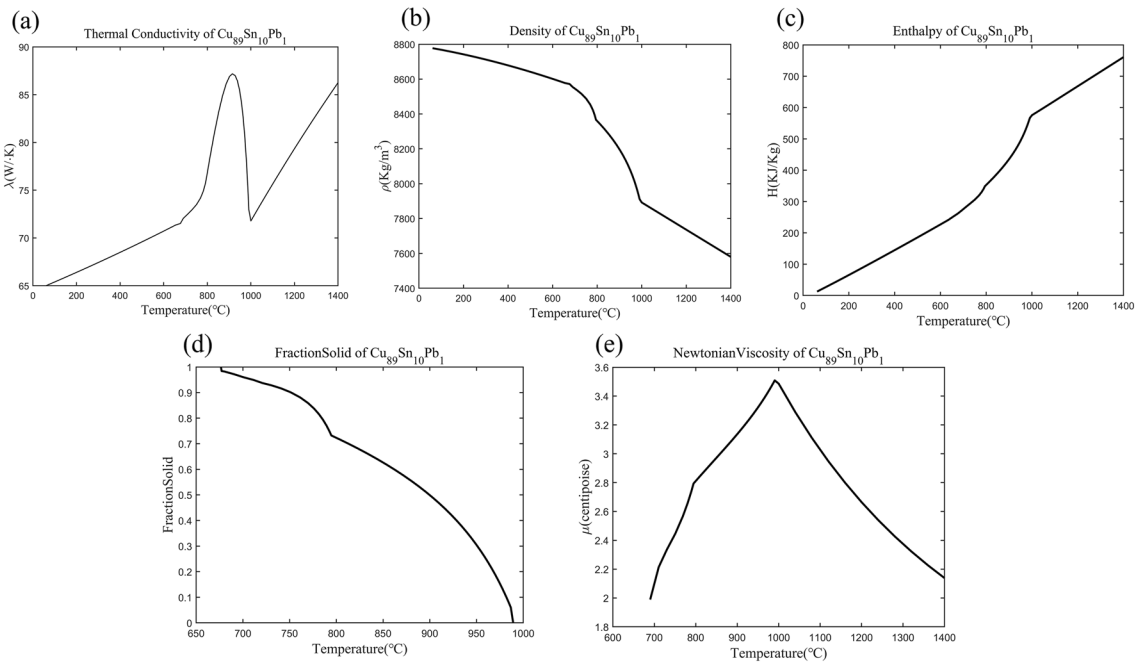

Fig. 3 System-generated thermophysical properties of the metal body (89% Cu, 10% Sn, and 1% Pb). **a** Conductivity; **b** density; **c** enthalpy; **d** fraction solid; **e** viscosity

Table 2 Core diameters in casting simulation

Serial number	a	b	c	d	e	f
Metal core diameter (mm)	0	6	8	10	12	14

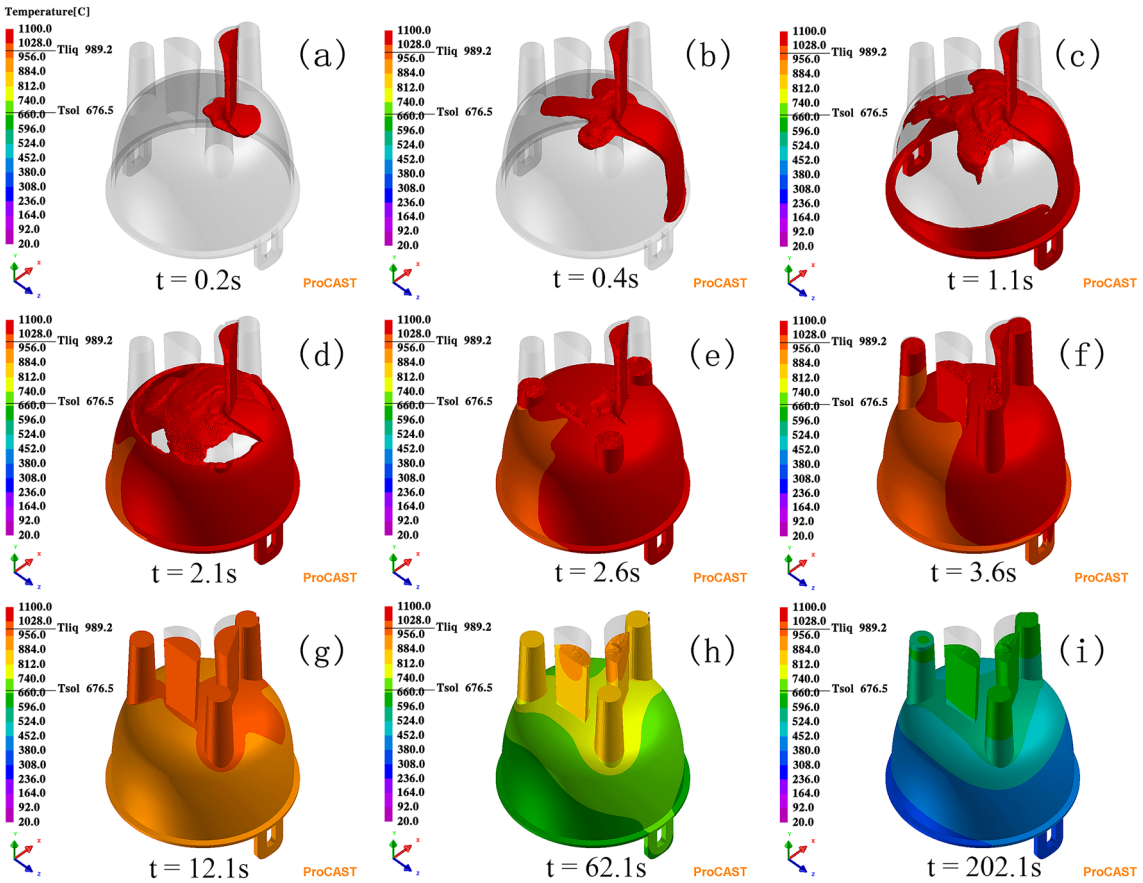

Fig. 4 Filling and solidification process of bronze casting simulated in ProCAST software (blank control). The color bars indicate the temperature distribution of alloy at different times

Results and discussion

Metal core and solidification time

Figure 5 displays the color maps reflecting solidification times of the legs for metal cores with different diameters. This value displays the time difference between the time to reach the solidus temperature and the time to reach the liquidus temperature. The legs without the metal cores (orange areas in Fig. 5a) require about 147–158 s for solidification. When a metal core with a diameter of 6 mm is adopted, the solidification time of the leg decreases to 125–136 (light green circles in Fig. 5b).

It is evident that the solidification time is proportional to the diameter of the metal core (Fig. 5c, e). The largest diameter (14 mm) corresponds to the shortest solidification time (26 s in Fig. 5f), indicating that the use of metal core can greatly reduce the solidification time. Although the oversized metal core (Fig. 5f) leads to fast solidification, it also has the risk of blocking the pouring channels and thus leading to casting defects.

Therefore, the solidification time of the leg was reduced by almost 100 s from the blank control to the metal core with a 10 mm diameter, showing the most obvious casting effect. From the perspective of micro-structure, the reduction of solidification time leads to structural changes of specific parts of the casting at the micro-level. According to Formula 1, shortening the solidification time of the legs will reduce the diameter of the secondary dendrite arm, resulting in finer dendrites. A decrease in the solidification time from 160 to 60 s (i.e., almost by 2/3) induces a decrease in the secondary dendrite arm diameter by about one third, which can significantly improve the performance of the casting [29]. This indicates that the use of metal core can improve and optimize the structure of the bronze to a large extent.

Metal core and casting hot spots

In order to further verify the function of the metal core, the influence of metal core size on the hot spots of bronze casting was simulated.

In the blank control group, the legs appeared orange, meaning that the time for hot spots to reach the critical solid fraction was about 86.67–93.33 s (Fig. 6a). Once a 6 mm metal core was adopted, the color changed to yellow and light green, indicating the time for hot spots

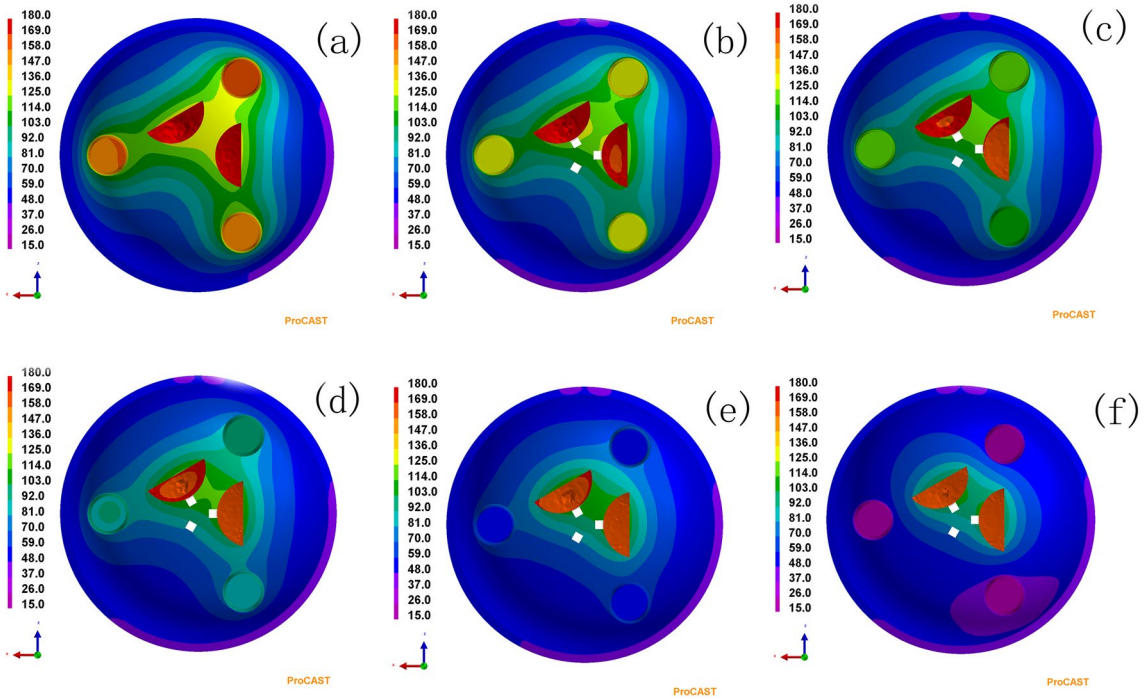

Fig. 5 Influence of metal core diameter on the solidification time of bronze, simulated in ProCAST environment. The color bars indicate the solidification time. (**a** blank control; **b** 6mm metal core; **c** 8mm metal core; **d** 10mm metal core; **e** 12mm metal core; **f** 14mm metal core)

to reach the critical solid fraction was 60.00–73.33 s (Fig. 6b). When the diameter of the metal core was increased to 10 mm, the critical solidification time of hot spots was reduced below 33.33 s (Fig. 6d). Finally, applying the metal core with the diameter of 12 mm eliminated the hot spots (Fig. 6e). According to the figures, the hot spots in the legs gradually decreased and vanished, but emerged again in group (f). The same pattern was also observed for the body of the vessel (Fig. 6). Due to the excessive chill effect caused by the excessive metal core size, the tripod legs quickly solidified to form multiple closed areas, and the feeding channels were blocked, forming isolated hot spots. Therefore, it can be reasonably concluded that appropriate size of the metal core plays an important role in controlling the hot spots during the casting process. The hot spots are correlated with casting defects [30–32].

Metal core and casting defects

In view of the above considered effect of metal core size on the solidification time and hot spots of the vessel, the quality of the final solidification product, casting defects, especially the possible presence of total shrinkage porosity, can be further assessed. In this regard, the next step was dedicated to simulate the influence of metal core diameter on the casting defects of bronze, such as shrinkage porosities. According to the results of the blank control group (Fig. 7), shrinkage porosities were observed in the legs, ears, gate and riser. When the 6 mm metal core was applied, all the shrinkage porosities in the ears vanished. Moreover, the shrinkage porosities decreased with the increase in metal core diameter, implying that this design could significantly reduce shrinkage porosities under the same casting conditions. However, when the size of the metal core exceeded a certain value, the shrinkage porosities were reproduced (Fig. 7f). The most pronounced effect was achieved when the size of the core was between 10 and 12 mm; shrinkage porosities were only found in the gate and riser of the bronze, while being eliminated from the body (Fig. 9d, e).

Figure 8 displays the simulated relationship between the value of total shrinkage porosity and the metal core diameter. It can be seen from the figure that, compared with the blank control (with reference to the 0 mm diameter of the metal core in Fig. 8), the lowest level of shrinkage porosity is achieved with core of 10 mm diameter (about 60%). However, with further increase in the core diameter, the porosity volume rises slightly, and once the metal core diameter reaches 14 mm, shrinkage porosity is observed again at the bottom of the legs.

The simulation results show that the metal core plays an essential role in casting. In particular, the use of a 10 mm metal core basically eliminates the hot spots in the legs, which also reduces the shrinkage porosities in the

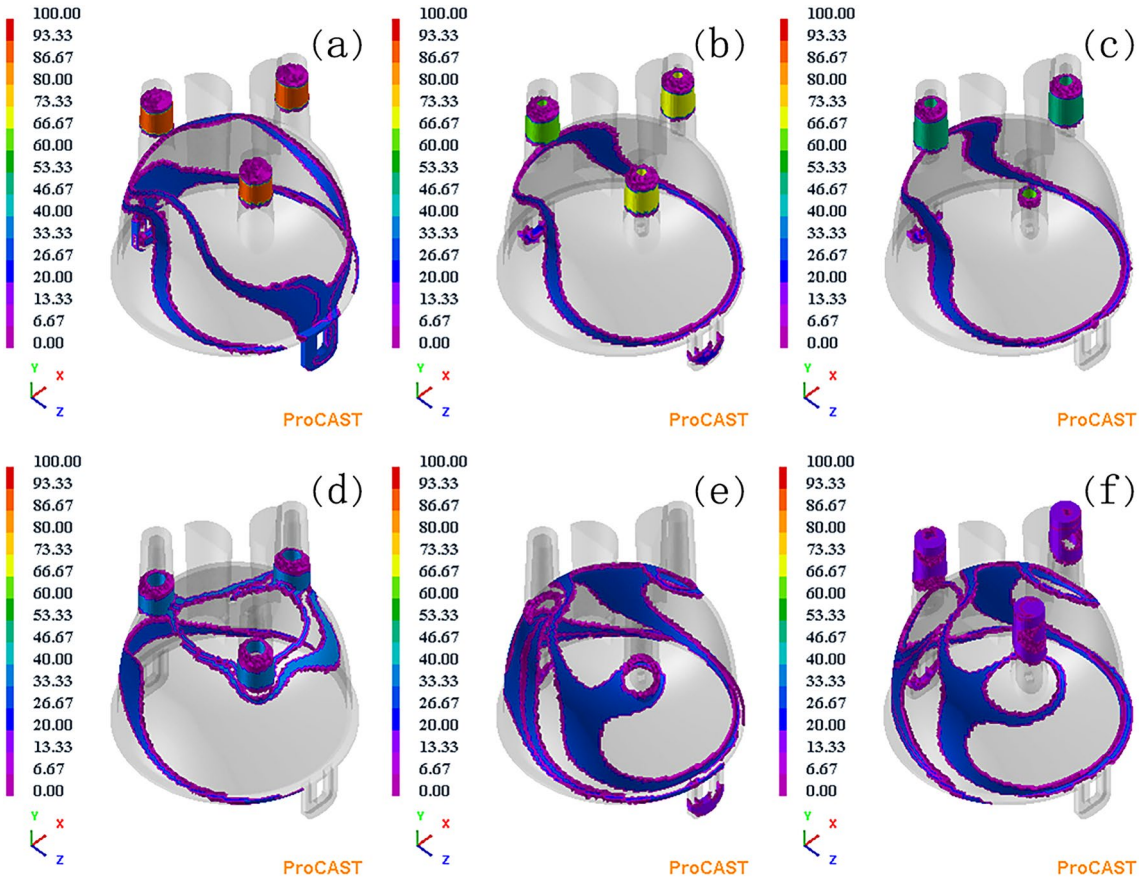

Fig. 6 Effect of metal core diameter on hot spots in bronze casting. The color bars indicate the regions around a local maximum point of solidification time and time maps when the local maximum point reaches the critical solid fraction. (**a** blank control; **b** 6mm metal core; **c** 8mm metal core; **d** 10mm metal core; **e** 12mm metal core; **f** 14mm metal core)

whole bronze by about 60%, so that the remaining defects are concentrated in the gate and riser. After removing these parts from the bronze in the post-casting process, a defect-free high-quality product can be obtained. However, the metal core diameter should not exceed a certain value [32, 33]: when the metal core size is above a certain value, the liquid alloy will solidify too fast to obtain feeding, thus producing new shrinkage porosity defects [34].

Comparative analysis of simulated casting results between metal core and clay core of the same size

In order to further clarify the function of metal core in defect control of the cast, metal cores with the above established optimal sizes of 8, 10, and 12 mm were chosen for comparison with clay cores of the same dimensions. As seen from the simulated images of clay cores (Fig. 9a, c) and metal cores (Fig. 9d, f), when the diameters in both cases are 8 and 10 mm, more precise control of shrinkage porosities is achieved by the metal core. At 10 mm, the shrinkage volume control of the metal core is clearly more effective than that of clay (Table 3).

However, regardless of the material used, since the core cannot be taken out after casting, there always exists a risk of cracking in the legs due to different shrinkage rates between the core and the bronze body. While the shrinkage rate of bronzes varies slightly according to the copper-tin-lead ratio used in a certain case, the overall shrinkage rate is about 1.9%. In turn, the shrinkage rate of clay mold is roughly 0.9% [35]. For example, the M9:14 bronze tripod unearthed from Zhouyuan Site with reference to the Early Western Zhou Dynasty period (ca. 1045–975BCE) contained clay cores in its legs (Fig. 10a), and one leg exhibited obvious signs of splitting (Fig. 10b). When using metal core, similar defects can be avoided to a large extent because of almost equal shrinkage rates of the core and the body.

According to the research conducted by Yang Huan [6], in Shang and Zhou periods, the craftsmen adopted clay cores, usually in the ears and legs of vessels, in order to maintain equal wall thickness of the bronze and achieve high-quality tripods. From the simulation casting in this work, the metal core can also achieve

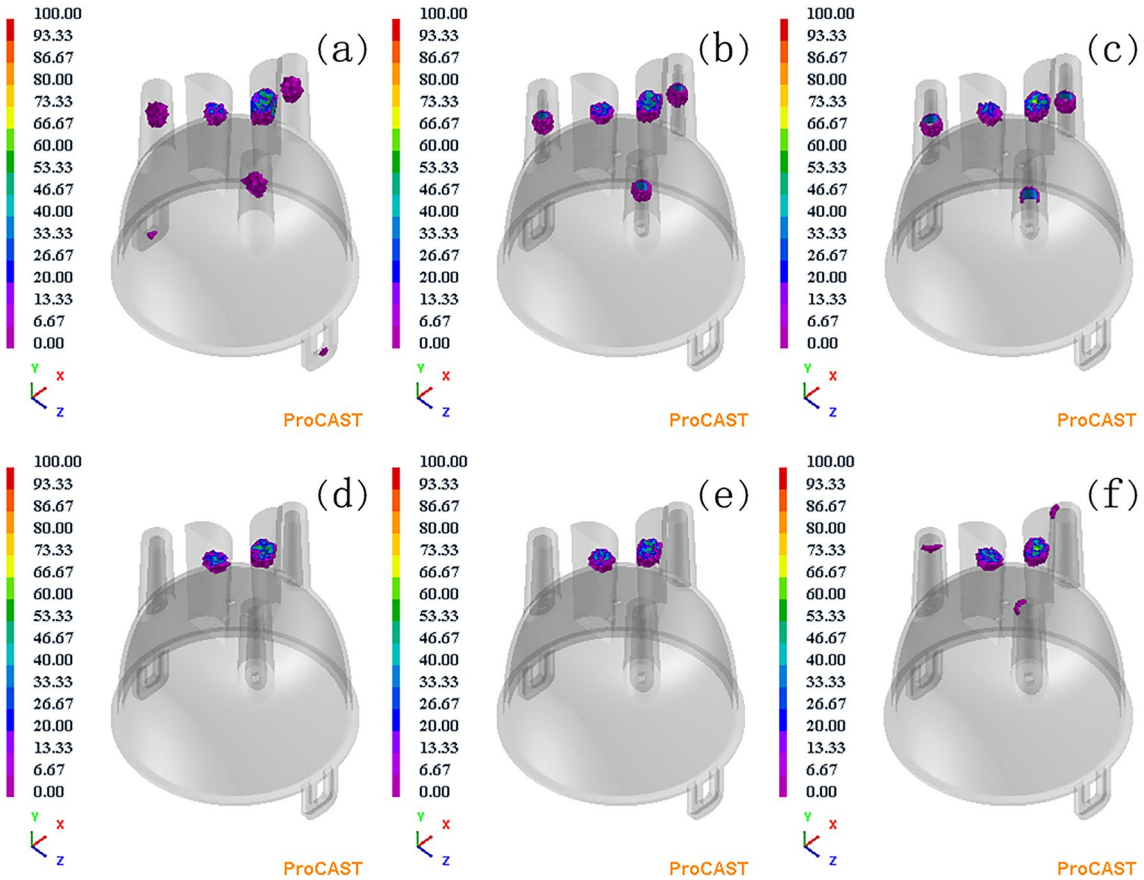

Fig. 7 Influence of metal core diameter on casting defects in bronze. The color bars indicate the distribution and volume of total shrinkage porosity, where the change from red to purple corresponds to the value of total shrinkage porosity from 100–0% (**a** blank control; **b** 6 mm metal core; **c** 8 mm metal core; **d** 10 mm metal core; **e** 12 mm metal core; **f** 14 mm metal core)

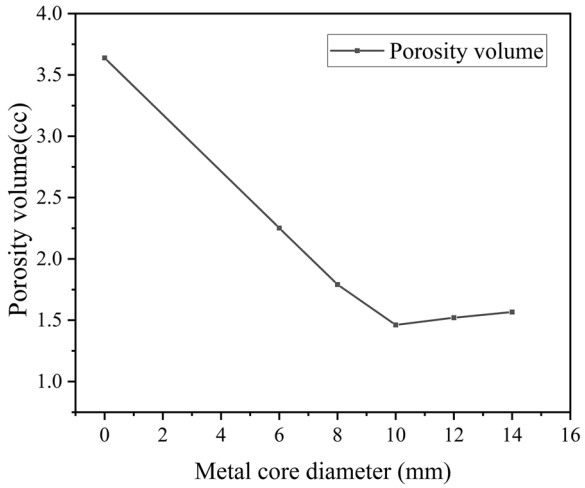

Fig. 8 Relationship between porosity volume and metal core diameter

the design of equal wall thickness. In addition, the metal core can shorten the solidification time of the bronze, refine the grains, and reduce the casting defects, such as shrinkage cavities and porosities.

Compared with the clay core, the metal core can play the role of casting chill to some extent due to the possibility of decreasing casting hot spots and preventing the formation of casting defects. In addition, according to Garbacz-Klempka, when casting with high humidity clay cores, several defects in casting structures were noticed during X-ray flow detection tests [14]. However, there is no humidity problem when using metal cores. Finally, the thermal expansion coefficient of the metal core differs from that of the clay core while being closer to the shrinkage rate of the body. Consequently, the use of metal core can reduce the cracks in the vessel caused by different shrinkage rates, so as to obtain a more resistant vessel.

Table 3 Relationship between the core material and casting defects

Material of the leg core	Clay core			Metal core		
Diameter of the leg core/mm	8	10	12	8	10	12
Volume shrinkage/cm^3	4.391	3.730	2.594	3.663	2.511	2.557
Volume of shrinkage cavity and porosity/cm^3	2.244	1.691	1.504	1.791	1.496	1.520

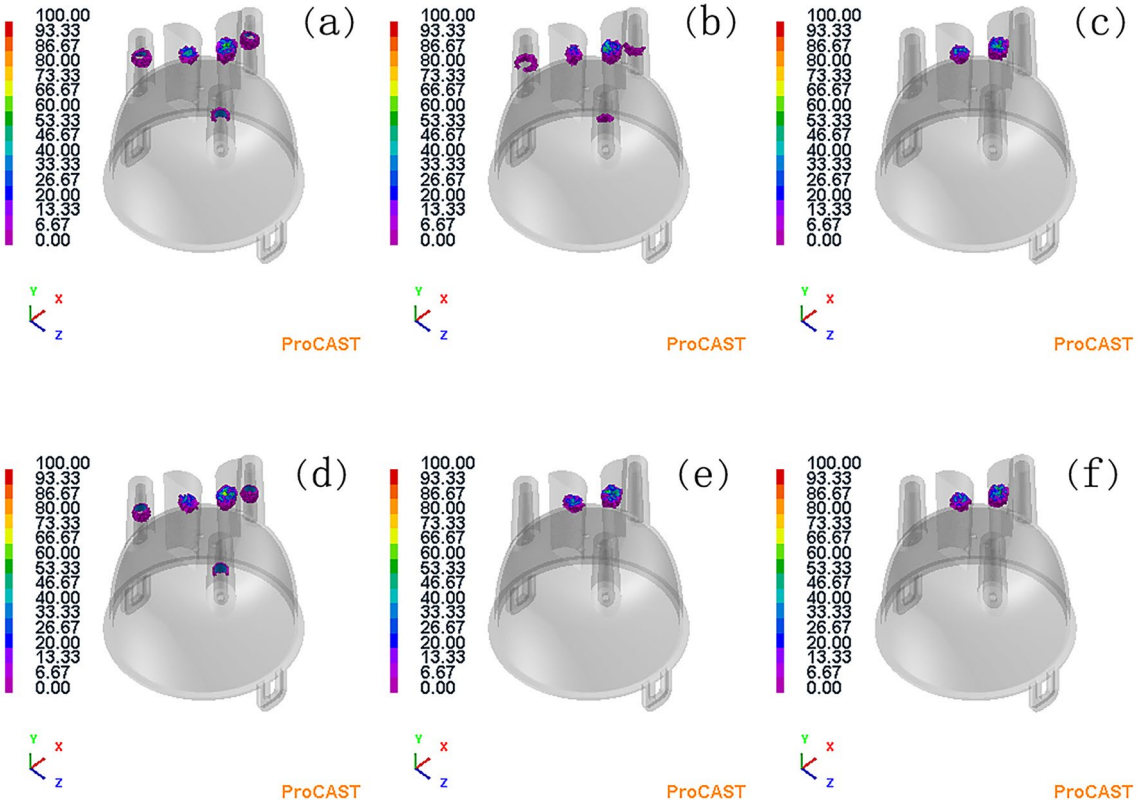

Fig. 9 Comparison of simulated shrinkage porosity in clay and metal cores. The color bars indicate the value of total shrinkage porosity, where the change from red to purple corresponds to the value of total shrinkage porosity from 100 to 0% (**a** 8 mm clay core, **b** 10 mm clay core, **c** 12 mm clay core, **d** 8 mm metal core, **e** 10 mm metal core, **f** 12 mm metal core)

Conclusion

The systematic observation and solidification simulation of metal cores of a bronze tripod showed that using metal cores of reasonable size in the legs of the ancient vessel effectively reduced casting hot spots and thus played the role of casting chill. In particular, the amount of total shrinkage porosity in core-containing vessels during solidification can be reduced by more than 60%.

When the clay core is used to maintain equal wall thickness of ears and legs, the difference in shrinkage rates between the core and the body of the vessel increases the possibility of leg cracking by the clay core with insufficient concession. Although the metal core cannot completely prevent this defect, it can suppress the occurrence of leg cracks.

The use of metal cores also poses some risks due to their obvious chill effect. When the core size exceeds a certain value, it will cause the priority solidification of the surrounding alloy liquid, thus blocking the flow channel. The examination of seven tripods with metal cores revealed the complete formation of their legs without any shortage of pouring, indicating that the craftsmen at that time mastered the size and composition of the cores to achieve exquisite bronze casting.

Moreover, the metal cores within the bronze legs with reference to the late Shang and early Zhou dynasties had

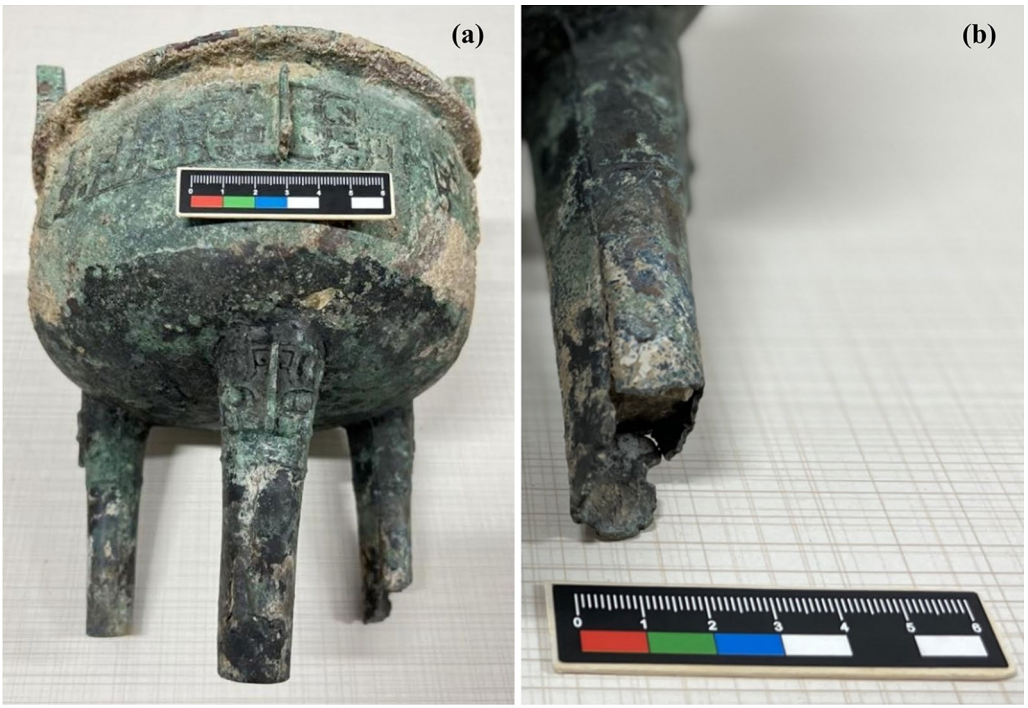

Fig. 10 Legs with clay cores and casting defects of M9:14 tripod unearthed from Zhuangli foundry in Zhouyuan, referred to Western Zhou Dynasty period. **a** Full picture of tripod M9:14, **b** leg of tripod M9:14

many more functions than just reducing casting defects as previously thought. Specifically, the metal cores not only facilitated equal thickness of the body wall, but also served as important casting chills in the legs that were prone to casting defects. At present, most tripods with metal cores in their legs possess a complete shape, exquisite pattern, and reasonable composition ratio, showing a fairly high level of casting technique. In general, metal cores appear to provide an "optimal solution" to avoid casting defects and achieve equal wall thickness.

Since the tripod legs with metal cores are not easy to distinguish from conventional solid legs via X-ray and CT detection methods and this topic has not yet attracted much attention of researchers, the number of vessels found is still relatively small. It is believed that with the advancement of detection technology, more tripods with metal cores will be found in the future. Moreover, further research is needed to elucidate the origin and principles of this unique technology, in order to draw a more comprehensive conclusion.

Acknowledgements
The authors are grateful to the State Key Laboratory of Solidification Technology of Northwestern Polytechnical University for their methodological supporting on the solidification simulation.

Author contributions
HY, MF and YC conceived the study. RL and ZF did sample selection. MF and ZF performed laboratory work and data analysis. HY wrote the original draft. MF prepared figures. JY served as an academic adviser on the article. HY collected archaeological data. All authors commented and edited the manuscript.

Funding
This article is supported by the Chinese National Social Science Fund under the project: 'Comparative Research on the Construction Technology of Pre-Qin Bronze Chariots of China' (Project Number: 18XKG001).

Availability of data and materials
The data and materials are available from the corresponding author on reasonable request.

Declarations

Competing interests
The authors declare no competing interests.

Received: 6 July 2023 Accepted: 20 November 2023
Published online: 01 December 2023

References

1. Wang T. Chinese bronzes from the Meiyintang collection. London: Paradou Writing Ltd; 2009.
2. Yetts WP. Catalogue of the Chinese and Korean bronzes. In: Hopkins LC, editor. The George Eumorfopoulos collection, vol. I. London: Ernest Benn, Ltd. Bouverie House; 1929. p. 36–8.
3. Karlbeck O. Anyang molds. Bulletin—the Museum of Far Eastern Antiquities (Ostasiatiska Museet) Stockholm, vol. 7. Sweden: The Museum; 1935. p. 39–60.

4. Rutherrord J, Gettens SI. The freer Chinese bronzes volume II technical studies, Smithsonian Institution Freer Gallery of Art. Washington: Smithsonian Publication 4706; 1969.
5. Izumiya Museum Izumi House Bogokan. Quanwutoushang, scanning and analysis of bronzes in Izumi House Bogokan. Beijing: Science Press; 2015. p. 461 (**in Chinese**).
6. Lian W, Wei B, Fan JH. Changing hot spot of casting and the position relationship between riser and hot spot. Foundry Technol. 2004;11:811–2 (**in Chinese**).
7. Liao Q, Ge P, Lu GX, et al. Simulation study on the investment casting process of a low-cost titanium alloy gearbox based on ProCAST. Adv Mater Sci Eng. 2022. https://doi.org/10.1155/2022/4484762.
8. Yang H, Jiang L, Yang JC, Chen YZ. Uniform wall thickness on ancient Chinese bronzes: a post-casting perspective. Jianghan Archaeol. 2022;5:108–16 (**in Chinese**).
9. Bamberger M, Minkoff I, Stupel MM. Some observations on dendritic arm spacing in Al-Si-Mg and Al-Cu alloy chill castings. J Mater Sci. 1986;21:2781–6.
10. Mi GF, Liu XY, Zhu ZJ, et al. Effects of chill casting processes on secondary dendrite arm spacing and densification of Al-Si-Mg alloy. Trans Nonferr Met Soc China. 2007;17(5):1012–7.
11. Wankhede DM, Narkhede BE, Mahajan SK, et al. Experimental investigations of mechanical properties and microstructural characterization of aluminum–silicon alloy castings. In: International conference on intelligent manufacturing and automation (ICIMA); 2018. p. 267–77.
12. Meyers P, Holmes LL. Technical studies of ancient Chinese bronzes: some observations. 1983.
13. Liu R, Pollard AM, Cao Q, et al. Social hierarchy and the choice of metal recycling at Anyang, the last capital of Bronze Age Shang China. Sci Rep. 2020;10:18794.
14. Yang H. A research on lead content of the freer Chinese bronzes in Shang Dynasty. Jianghan Archaeol. 2017;3:130–6 (**in Chinese**).
15. Chase WT. Ancient Chinese bronze art–casting the precious sacral vessel. New York City: China House Gallery China Institute in America; 1991. p. 32.
16. Lian HP. The application of metal cores in the casting of bronze tripods in the late Shang Dynasty-early western Zhou Dynasty. In: Henan Provincial Institute of Cultural Heritage and Archaeology, editor. Researches on Shangzhou bronze casting process. Beijing: Science Press; 2019. p. 203–7 (**in Chinese**).
17. Garbacz-Klempka A, Karczmarek L, Kwak Z, et al. Analysis of a castings quality and metalworking technology. Treasure of the bronze age axes. Arch Foundry Eng. 2018;18(3):179–85.
18. Hassan I, Sheikh AK, Al-Yousef AH, Younas M. Mold design optimization for sand casting of complex geometries using advanced simulation tools. Mater Manuf Process. 2012;27(7):775–85.
19. Riposan I, Stan S, Chisamera M, Neacsu L, Cojocaru AM, Stefan E, Stan I. Control of solidification pattern of cast irons by simultaneous thermal and contraction/expansion analysis. IOP Conf Ser Mater Sci Eng. 2019;529(1):012016.
20. da Silva Albuquerque CE, Grassi END, De Araújo CJ. Castability of Cu-Al-Mn shape memory alloy in a rapid investment casting process: computational and experimental analysis. Int J Adv Manuf Technol. 2023;127:2563–79.
21. Abdullin AD. Detecting microporosity defects in steel castings by computer modeling of the casting operation in ProCAST. Metallurgist. 2013;57:167–71.
22. Yang H, Jiang L, Fang Z, Fang M, Yang JC, Chen YZ. Research on the mechanism of solidification and related technical problems of ancient Chinese bronzes. Sci Conserv Archaeol. 2022;34(6):127–38 (**in Chinese**).
23. Liu N. Hydrodynamic analysis of the Interaction between ship and broken ice. Dalian: Dalian University of Technology; 2021. p. 4–8 (**in Chinese**).
24. Lu Y. Predicting and validating multiple defects in metal casting processes using an integrated computational materials engineering approach. Columbus: The Ohio State University; 2019. p. 4–5.
25. Rao L, Zhu LB, Hu QY. Finite element mesh model analysis and model information transform method in casting simulation process. AMM. 2012;217–219:1618–21.
26. Cho IS, Kwak SY, Kim YH et al. Effect of cooling rate on the porosity defect in the thick aluminum casting by 3D computed tomography analysis. In: Joint conference of 5th international conference on advances in solidification processes (ICASP) and 5th international symposium on cutting edge of computer simulation of solidification, casting and refining (CSSCR); 2019.
27. Zhang W, Liu L, Zhao X, et al. Effect of cooling rates on dendrite spacings of directionally solidified DZ125 alloy under high thermal gradient. Rare Met. 2009;28:633–8.
28. Zhang Y, Ma TJ, Xie HX, et al. Estimating the cooling rates of a spot welding nugget in stainless steel. Weld J. 2012;91(9):247-s–51-s.
29. Li Y, Liu JX, Zhang Q, Huang WQ. Casting defects and microstructure distribution characteristics of aluminum alloy cylinder head with complex structure. Mater Today Commun. 2021;27: 102416.
30. Elmquist L, Diószegi A. On the problems of a migrating hot spot. MSF. 2010;649:443–8.
31. Choudhari CM, Narkhede BE, Mahajan SK. Methoding and simulation of LM 6 sand casting for defect minimization with its experimental validation. Procedia Eng. 2014;97:1145–54.
32. Seo H-Y, Seo P-K, Kang C-G. A study on the S/W application for a riser design process for fabricating axisymmetric large offshore structures by using a sand casting process. Int J Naval Archit Ocean Eng. 2019;11(1):462–73.
33. Chang QM, Yuan J, Yang YK, Chen X. Modeling analysis and optimization of sand casting process. AMR. 2012;479–481:226–9.
34. Wang Y, Gao MQ, Yang BW, et al. Microstructural evolution and mechanical property of Al–Mg–Mn alloys with various solidification cooling rates. Mater Charact. 2022;184: 111709.
35. Tan DR, Xu HK, Huang L. A study of the techniques of bronze casting with clay molds in Bronze Age China. Acta Archaeol Sin. 1999;2:211–50 (**in Chinese**).

Publisher's Note